DYNAMICAL AND PHYSICAL PROPERTIES OF 65803 DIDYMOS. D. C. Richardson[1], O. S. Barnouin[2], L. A. M. Benner[3], W. F. Bottke Jr.[4], A. Campo Bagatin[5], A. F. Cheng[2], M. Hirabayashi[6], C. Maurel[7], J. W. McMahon[6], P. Michel[8], N. Murdoch[7], S. P. Naidu[3], P. Pravec[9], A. S. Rivkin[2], D. J. Scheeres[6], P. Scheirich[9], K. Tsiganis[10], Y. Zhang[1,11], and the AIDA Dynamical and Physical Properties of Didymos Working Group[12], [1]Department of Astronomy, University of Maryland, College Park, MD 20742, dcr@astro.umd.edu, [2]JHU/APL, [3]JPL/Caltech, [4]SwRI, [5]U Alicante, [6]U Colorado, [7]ISAE, [8]Obs. Côte d'Azur, [9]Acad. Sci. Czech Rep., [10]Aristotle U, [11]Tsinghua U, [12]various.

Introduction: The near-Earth asteroid (NEA) 65803 Didymos, a binary system, is the target of the proposed Asteroid Impact & Deflection Assessment (AIDA) mission, which combines an orbiter [1] and a kinetic impactor experiment planned for fall 2022 [2]. The Dynamical and Physical Properties of Didymos Working Group is supporting this mission by addressing the following broad questions: what is the dynamical state of the Didymos system, how can the consequences of the impact best be measured, and how can the physical properties of the system be inferred based on current knowledge? Below we outline our current progress toward answering these questions.

Origin: Didymos is an Apollo-class NEA with semimajor axis, eccentricity, and inclination (a, e, i) of (1.64 AU, 0.384, 3.4°). Using a new NEA population model [3], it likely reached its current orbit by exiting the inner main belt near or within the ν_6 resonance between 2.1–2.5 AU (> 82%). Other possible source regions are the Hungaria asteroids (8%) and the inner/central main belt via the 3:1 mean-motion resonance with Jupiter (7%). Remote observations [4] show Didymos is spectroscopically most consistent with ordinary chondrites, with an affinity for L/LL-type meteorites. Didymos likely originated from a high-albedo family [5]; its geometric albedo, p_v = 0.16 ± 0.04 [6], matches the mean albedo of the prominent Baptistina family in that zone. However, several additional family candidates may also make plausible parents (e.g., Flora, Nysa, Massalia, Lucienne).

Current Dynamical State: Table 1 gives basic data on the current dynamical and rotational state of Didymos based on observations to date. The secondary is assumed to orbit in the equatorial plane of the primary. Figure 1 shows the current shape model from radar and lightcurve observations. Also see [7].

Table 1: Didymos System Basic Properties

Primary Diameter	0.780 ± 10% km
Secondary Diameter	0.163 ± 0.018 km
Total System Mass	$(5.278 \pm 0.04) \times 10^{11}$ kg
Component Bulk Density	2,100 km m^{-3} ± 30%
Primary Rotation Period	2.2600 ± 0.0001 h
Component Separation	1.18 +0.04/−0.02 km
Secondary Orbital Period	11.920 +0.004/−0.006 h

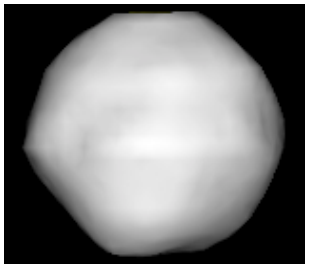

Figure 1: Preliminary shape model of the primary from combined radar and lightcurve data, diameter ~780 m. The secondary (not imaged) is estimated to be more elongated.

System dynamics. We have constructed a model for the short-term binary dynamics in which each component is represented by a rigid body composed of ~1,000 blocks that fit its shape. The secondary is assumed to be a triaxial ellipsoid, with axial ratios a/b and b/c varying between 1.1 and 1.5. Almost all cases appear to be stable for 500 orbits, in the absence of solar tides. The orbital period and semimajor axis have very small variations (~1 m) and the eccentricity of the orbit stays < 0.018, increasing slightly with a/b and b/c. The orbital plane oscillates minimally about the initial one (i < 0.003°). The rotation axes remain stable, as the obliquity stays < 0.02° and < 0.3° for the primary and secondary, respectively. While the rotation period of the primary is extremely stable (δP_1 ~ 0.1 s), the secondary shows secular oscillations—possibly librations—that depend on the axial ratios and may range from δP_2 ~ 0.2 to 1.5 h. A more complete long-term analysis is currently underway.

Internal Structure: The Didymos primary is close to if not beyond the limit for loose material to remain on the surface at the equator. Weak cohesion (< 100 Pa) may be implied, although there is sufficient uncertainty in the shape model that zero cohesion cannot yet be ruled out.

Continuum analysis. Figure 2 shows the failure mode diagram of the primary (indicating the degree of cohesion needed to maintain its shape as a function of spin period), based on a continuum analysis [8], assuming uniform internal structure and the nominal bulk density. A Drucker-Prager model is used for the yield condition, and the friction angle is fixed at 35°. We find two distinct failure modes, if there is insufficient cohesion/friction. If Didymos fails at a spin period longer than 3.0 h, only the equatorial region fails. Otherwise, the internal structure should fail first.

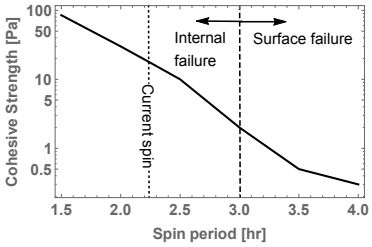

Figure 2: Didymos failure mode plot. The current spin period is 2.26 h; the boundary between surface failure and internal failure is ~3 h.

Discrete-element analysis. Using a soft-sphere approach [9,10] we are exploring the conditions needed for a rubble-pile model of the primary made up of monodisperse spheres to hold its shape. We find that gravel-like material properties (friction angle 40°) together with a spring-dashpot rolling friction model give a stable outcome without cohesion for bulk density > 2,500 kg m^{-3} when the spheres are packed randomly, and at even lower densities for hexagonal-close-pack configurations. The relative internal pressure distribution for a stable random-packed case is shown in Fig. 3. Analysis of this case shows that it is everywhere below the Drucker-Prager yield condition.

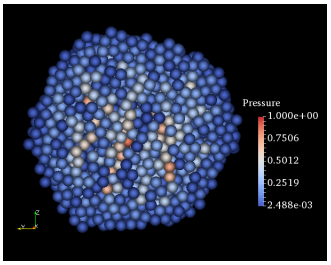

Figure 3: Relative pressure distribution in a stable discrete model of the spinning primary (cross section). Material repose angle ~37°, packing efficiency ~62%.

Long-term Perturbations: The impact is expected to change the orbital period of the Didymos secondary by several minutes (~1%). It is necessary to understand any natural perturbative effects that may mask the impact signal.

Effect of solar and Earth tides. The Sun will contribute the largest tidal effect on the system, but at a level 10 times below that anticipated for the impact itself. Formally, Earth tides can be slightly stronger than solar tides, but the necessary orbital configuration will not occur before or during encounter.

Thermal radiation forces. Thermal re-radiation from the Didymos secondary will lead to the binary-YORP (BYORP) effect [11], which can cause a long-term secular change to the binary semimajor axis. Without a detailed shape model of the secondary, we can use its estimated ellipsoid shape, and density and orbit properties from Table 1, to scale the BYORP rate from 1999 KW_4 [12]. This shows that if the deviation in the shape of the Didymos secondary from a perfect ellipsoid is similar to that of the 1999 KW_4 secondary, the Didymos orbit semimajor axis may grow/shrink at ± 1.66 cm yr^{-1}. This translates to a mean quadratic anomaly drift rate of ± 2.8° yr^{-2}, or a very small period drift of 0.91 s yr^{-1}. If the BYORP effect is working to shrink the binary orbit, intercomponent tidal forces can oppose the effect, resulting in a constant orbit size [13], as is hypothesized for 1996 FG_3 [14]. Further details about these processes and the resulting dynamical evolution for Didymos are discussed in [15].

Deploying a Lander: Using the ISAE-SUPAERO drop tower, we are performing low-speed collisions into granular material in low gravity to model a possible lander deployment on the Didymos secondary. The aim is to understand the acceleration profile upon impact and to quantify the coefficient of restitution if the lander bounces. Reduced gravity is simulated by releasing a free-falling projectile into a surface container with a downward acceleration less than that of Earth's gravity, controlled using an Atwood machine (a system of pulleys and counterweights). The projectile, sample container, release mechanism, and deceleration system are custom designed for the 5.5 m drop tower [16] and provide collision speeds and accelerations < 0.2 m s^{-1} and 0.1–1.0 m s^{-2}, respectively, lower than in previous experiments [17,18], and thus closer to the conditions that may be encountered during the AIDA mission.

Orbiting Debris: Due to the fast rotation of the primary and given the nominal physical parameters, centrifugal force may overcome gravitational force at low latitudes. That allows regolith material of any size to go through take-off/landing cycles and cause loss of fines due to solar radiation pressure. Analysis of this effect accounting for the current shape model is ongoing to estimate the effective mass density of floating material in the neighbourhood of the primary.

References: [1] Michel P. et al. (2016), *ASR*, submitted. [2] Cheng, A. F. et al. (2016) *P&SS*, accepted. [3] Granvik et al. (2015) *AAS/DPS*, mtg. #47, id. #214.07. [4] Dunn et al. (2013) *LPS XLIV*, Abstract #1197. [5] Nesvorný et al. (2015) *arXiv*, 1502.01628. [6] Pravec et al. (2006) *Icarus*, 181, 63–93. [7] Rivkin, A. S. (2016) *LPS XLVII*, submitted. [8] Hirabayashi M. and Scheeres D. J. (2015) *IAU Proc.*, 318, accepted. [9] Schwartz et al. (2012) *Gran. Matt.*, 14, 363–380. [10] Barnouin O. S. et al. (2015) *AAS/DPS*, mtg. #47, id. #402.09. [11] Ćuk M. and Burns J. A. (2005) *Icarus,* 176, 418–431. [12] McMahon J. W. and Scheeres D. J. (2010) *Icarus,* 209, 494–509. [13] Jacobson S. A. and Scheeres D. J. (2011) *APJL*, 736, L19. [14] Scheirich P. et al. (2015) *Icarus*, 245, 56–63. [15] McMahon J. W. et al. (2016) *LPS XLVII*, submitted. [16] Sunday C. et al. (2016) *Rev. Sci. Instr.*, submitted. [17] Goldman D. I. and Umbanhowar P. (2008) *Phys. Rev. E*, 77, 021308. [18] Altshuler E. et al. (2013) *arXiv*, 1305.6796.